Monitoring Strategy of Geological Hazards Using Integrated Three-dimensional InSAR and GNSS Technologies with Case Study

László Bányai[1], István Bozsó[1], Eszter Szűcs[1], Katalin Gribovszki[1*], Viktor Wesztergom[1]

[1] Institute of Earth Physics and Space Science, Csatkai E. u. 6–8., H–9400 Sopron, Hungary
* Corresponding author, e-mail: gribovszki.katalin@epss.hu

Abstract

Geodetic/geodynamic benchmarks, equipped with both ascending and descending radar corner reflectors, and a method for integrated InSAR and GNSS/GPS network observation were developed and applied as the continuation of the former geodetic monitoring at the Dunaszekcső landslide, Hungary. The attempts to apply InSAR technologies using archive and Sentinel-1 data practically failed on the most intensive landside areas ("Vár" and "Szent János" hills), where proper persistent or distributed scatterers were not found.

Our concept solved this problem, where the Simple Look Complex (SLC) images are used to interpolate the movements between two GNSS network observations using the integrated benchmarks and the method of Kalman-filtering.

Since the InSAR line-of-sight (LOS) changes are barely sensitive to the north movements, this information is essentially provided by GNSS measurement alone, moreover, the GNSS measurements are used to: a) identify the benchmarks, b) detect the unwrapping errors and missing cycles and c) provide the boundary values of Kalman-filtering.

After the installation of benchmarks three GPS observations were carried out and 69 ascending and 61 descending Sentinel-1 A and B images were processed.

The data processing properly indicated the general movement history, which fit the curves of former geodetic observations, as well. The dense data points of the East and Up (vertical) components made possible more detailed geomorphologic interpretations of the ongoing process between two GPS observations.

During the investigated periods the deceleration of movements was experienced, however, the deceleration of the dormant state needs the continuation of the monitoring.

Keywords

landslides, monitoring, InSAR and GPS/GNSS network

1 Introduction

The National Cadaster of Surface Movements [1] contains maps and descriptions of approximately 1,000 potentially dangerous areas in Hungary. One of the most exciting groups is the recurrent landslide along the right banks of River Danube, which are known since Medieval and Roman times. Over the last 2,000 years a bluff retreat of 5–15 m per 100 year was estimated by Lóczy et al. [2, 3].

During the last decades several studies were carried out to understand the ongoing processes of bank failures (e.g., [4–13]). These studies were performed usually after the main events applying geomorphological procedures.

The first published geodetic monitoring of a recent landslide was carried out in Dunaszekcső, nearly from the beginning of the reactivation in 2007 [14, 15]. Precise geodetic and GPS monitoring measurements were done using a network of stable and moving geodetic benchmarks. These investigations revealed the different phases of the landslide progress and indicated a correlation with groundwater level. The layers affected by higher groundwater table were able to move into the riverbed governing the speed of the dominantly sinking process.

Although this technology provides three-dimensional movements in mm level accuracy, the repeated measurements of the networks are very time consuming and expensive. These measurements were supported by scientific funds between 2007 and 2012. However, this landslide process is still active.

The application of permanent GNSS networks would provide even more accurate movement histories, but at a significantly higher cost, therefore it is not a reasonable choice.

The next promising technology is Satellite Radar Interferometry (InSAR), but at the beginning the purchase of SAR images was very expensive. Before ESA (European Space Agency) released the archive (ERS-1, ERS-2 and ENVISAT) images, the free access of data was connected to scientific project proposals. The advent of the ESA Sentinel-1 mission solved this problem, because the registered user could download the images free of charge.

InSAR seems to be a more convenient technique, where the processing of the images is carried out in the offices; however, the field validation of the result may be very important. Besides the advantages there are some limitations, as well. In the case of former ESA missions the revisit cycle was 35 day and the larger baselines caused a very fast decorrelation of interferograms in time and space. This problem is also solved by Sentinel-1 A and B satellites (revisit cycle is 6 day, and the diameter of the orbit tube is only 150 m). Furthermore, there are still vegetated areas, where proper persistent or distributed scatterers cannot be found.

InSAR technology can estimate accurate (1 mm – 1 cm) surface movements in satellite line-of-sight (LOS) directions along ascending (ASC) and/or descending (DSC) satellite passes, which are acquired in different epochs. The combination of ASC and DSC movements can estimate only vertical and east-west movements [16]. Additionally, there are only a few scatterers, which probably can be observed from both directions even over densely populated areas. Since InSAR is a double range technique the changes between two measurement epochs should be less than half wavelength (in case of Sentinel-1 ~28 mm), otherwise there are missing cycle in the time series.

In spite of the limitations there are numerous successful attempts to monitor landslides or other surface movements if optimal environmental conditions and proper data processing software are available (e.g., [17–27]). In these investigations usually geometric models of the investigated phenomenon (e.g., slope parameters) are used to compensate the geometric deficiency of ASC and DSC LOS movements.

There were also attempts to investigate the recent landslide area in Dunaszekcső using InSAR technology. During the international DORIS project [28] ERS-1, ERS-2, ENVISAT, ALOS and Terrasar-X images were analyzed. Unfortunately, proper scatterers were not found on the moving blocks. Only the processing of Terrasar-X images found four scatterers down at the foot of the moving bluff indicating 8-15 mm vertical sinking between May 2012 and Jan 2013 [29].

Sentinel-1 images were processed during the active period by Kovács et al. [30]. This investigation concentrated on the InSAR processing technology estimating average ASC and DSC velocities by ScanSAR software. Although Sentinel-1 images were processed, only two persistent caterers were found to the south of the most significantly moving part of the "Vár" hill area.

Considering our geodetic experiences and the characteristics of InSAR technology we designed and investigated integrated geodynamic/geodetic benchmarks together with a proper processing strategy supported by an ESA PECS project.

In the following sections, we shortly introduce this methodology, demonstrate the results of landslide monitoring of "Vár" hill area in Dunaszekcső and propose an optimal monitoring strategy for important and dangerous areas.

2 Methodology and the used devices
2.1 Study area and the monitoring network
In this study the "Vár" hill area of Dunaszekcső is investigated (Fig. 1), where former geodetic measurements [14, 15] and landslide fracture zone investigation [31, 32] were carried out by our institute.

There are numerous papers describing the geological and geomorphological setting of Dunaszekcső (e.g., [8, 30, 33–37]).
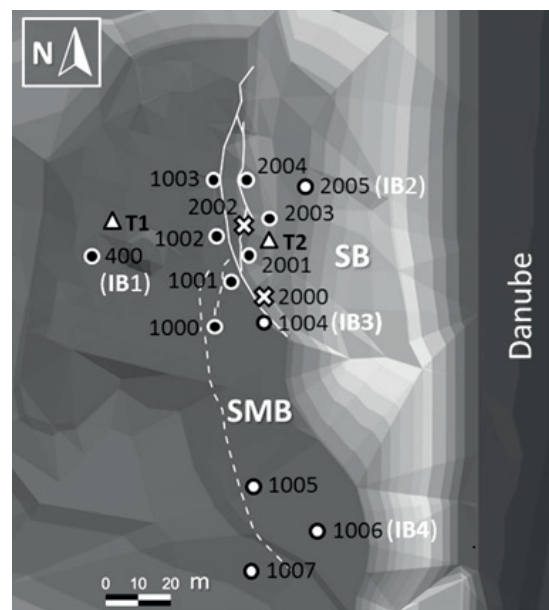
Fig. 1 The elevation model of "Vár" hill and the monitoring network in two blocks (SB and SMB). The black circles show the geodetic benchmarks of the first observation period while the new benchmarks are signed by white circles. The two triangles are the borehole tiltmeters and the name of collocated integrated benchmarks is given in brackets

The main characteristics of this area are shortly summarized. The basement is Jurassic limestone located at 200–250 m below the surface, which is covered by clayey and sandy sediments formed in the Upper Miocene and the Pliocene. These sediments are about 70 m deep under the "Vár" hill. The highest point is 142 m, and the nearly vertical loess wall (20–30 m) is above the former slopes (10–20 m), which consists of reworked loess from past landslides and fluvial mud, sand and gravel deposits of the Danube. The ground water is recharged from percolated rainfalls and the Lánka Stream, which resides in the lower part of the young and more porous loess deposits. These slopes can be recognized in Fig. 1, where the benchmarks of former geodetic investigations are also presented. The SB block is bounded by scarp edges (solid lines) of the intensive subsidence on 22.02.2008 (~6–8 m sinking in a few hours, which was corrected in the elevation model). The second block (SMB) started to move slowly in 2009 bounded by dashed lines.

To compensate the still present fast decorrelation in time of Sentinel-1 images caused by the environment, integrated geodetic benchmarks (IBs) were designed and installed at the study area. The theoretical and practical investigations of IBs are presented in Bányai et al. [38]. The 1 m^2 reinforced concrete basement of IBs holds truncated trihedral triangle corner reflectors (oriented to both ASC and DSC directions), reference adapter for geodetic/GPS measurements and other marks to control the possible tilt of the IBs at moving areas (Fig. 2). This arrangement assures the common application of ASC and DSC LOS series, which can be controlled by GNSS observations.
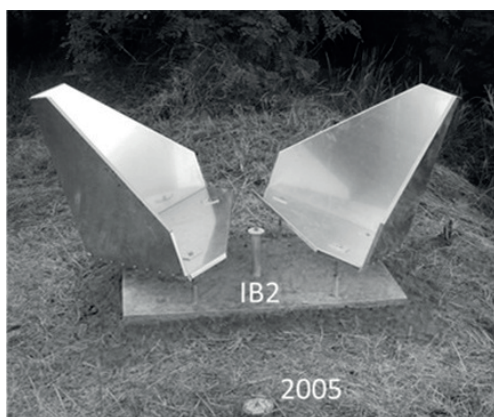

Fig. 2 One example of collocated traditional (2005) and integrated benchmark (IB2). The left and right corner reflectors are illuminated by ascending and descending SAR observations, respectively. The rod in the middle is the reference geodetic adapter. The relative positions of the phase centers and other marks are measured precisely to compute tilt corrections

The new monitoring network consists of the former reinforced concrete pillars placed on "stable" areas (points 100, 200, 300, 400 (Fig. 1) and 500). Close to the points 400, 2005, 1004 and 1006 four IBs were deployed in 2016 (Fig. 1). This ensures the continuity of the collocated benchmarks, since their relative positions were measured by GNSS in 2016. The points 2005, 1004 and 1006 were established in 2009 after the intensive subsidence episode. Their former GPS derived movements together with point 1000 were used for the interpretation of the results. All the GPS derived changes are shown in Fig. 3. Point 1000 started to move only after the intensive subsidence similarly to 1004 and 1006.

Despite the unfavorable circumstances the selected points can be measured properly by GPS/GNSS technique and can be illuminated by both ASC and DSC Sentinel-1 passes.

2.2 Data processing and the available data
In an early stage of InSAR applications one interferogram derived from two images were used to estimate the relative line-of-sight (LOS) changes. This technology provided very useful information in areas of large earthquakes and volcanos characterized by very low spatial and temporal decorrelation. In subsequently developed processing methods a stack of interferograms were used to
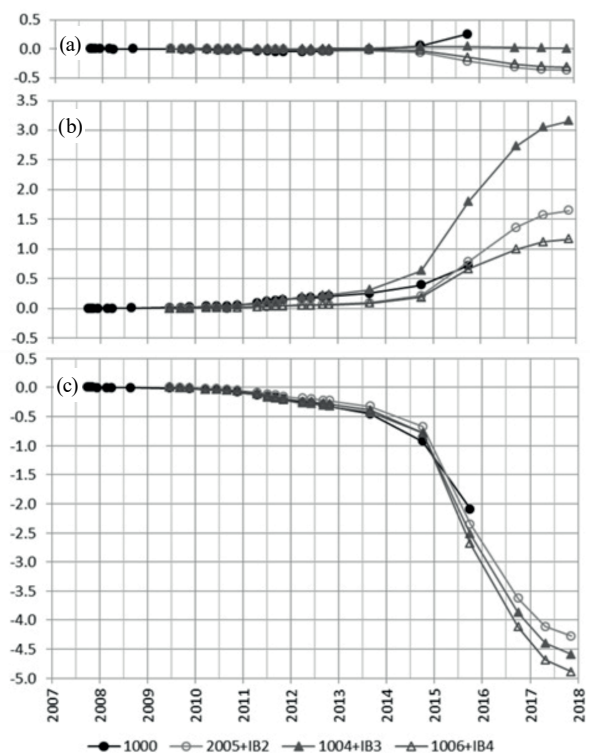
Fig. 3 GPS derived coordinate changes (m); North (a), East (b), Up (c)

derive average LOS displacement velocities, where averaging was used to filter the error sources. In recent times the different versions of Persistent Scatterer and/or Small Baseline Interferometry are the preferred method, which select and process only those pixels, which possess a selection of preliminary requirements (e.g., high coherence and low phase noise). In addition to the average velocities, the LOS time series are also provided.

Based on the integrated benchmarks we have developed the ISIGN (Integration of Sentinel-1 Interferometry and GNSS Networks) procedure and software package [39]. The computation process is based on the geo-referenced "normalized power", "coherence" and "diff" images preprocessed by the Gamma DIFF&GEO software [40]. The LOS displacements series are estimated by StaMPS/MTI (multi-temporal InSAR) software, which does not require a preliminary deformation model [41]. The pixels dominated by IBs are identified using the normalized power images and the GPS derived positions.

The ASC displacements are interpolated in the epochs of DSC data and vice versa, together with the epochs of starting and closing GNSS observations. The differences of ASC and DSC LOS displacement series (computed between "stable" IB1 and "moving" IB2-4 points) are processed by Kalman-filter estimating north, east and up components together with their instantaneous velocities. In this strategy the displacements between two GNSS measurements are interpolated using ASC and DSC LOS data, therefore the number of GNSS measurements can be limited to a reasonable level.

During this investigation the tilt measurements and the GPS network observations were carried out in 28.09.2016, 26.04.2017 and 08.11.2017. Altogether 69 ascending (between 2016.09.12 and 2017.11.18) and 61 descending (between 2016.09.16 and 2017.11.16) Sentinel-1 A and B images were processed. Three bursts of one Sub-Swath (IW1 or IW2) of the SLC images were selected, which cover the investigated area. No multilooking was applied and only the pixels dominated by IBs were processed by ISIGN. According to the ratio of average normalized pick power of selected pixels and their near background 0.3 mm precision of LOS data can be expected [38]. The computations were carried out in two intervals.

3 Results

For the demonstration of capabilities of integrated benchmarks the averaged and normalized ASC and DSC power images are presented between 26.04.2017 and 08.11.2017

in Fig. 4. It is clearly visible that the pixels of peak powers are dominated by IBs producing ghost scatterers in the nearby pixels, as well.

The numeric identification is carried out in one step using combination and permutation calculation, which is based on the minimum dispersion of the distances between the candidate pixel and GPS derived positions. The small differences of identified pixel positions are the consequence of different geometric positions of ASC and DSC master image and the errors of SRTM elevation model applied during the georeferencing of images.

The LOS displacement series and velocities estimated by StaMPS are basically referenced to the mean value of the whole investigated area. As usual in InSAR processing

(a)

(b)
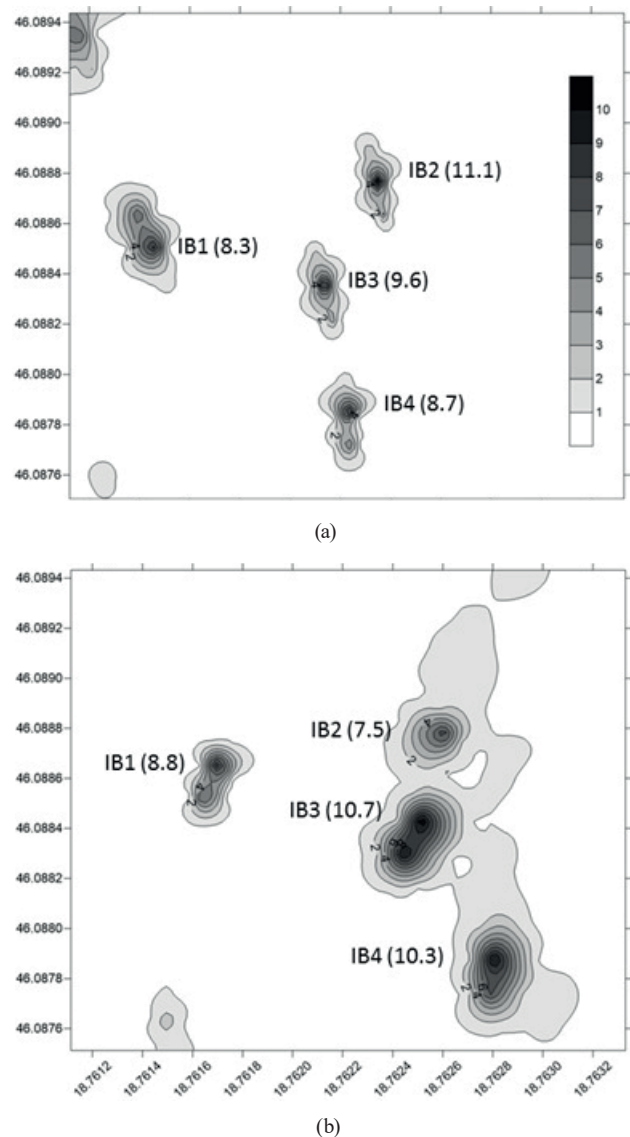
Fig. 4 The average ascending (a) and descending (b) normalized power images between 26.04.2017 and 08.11.2017 given in geographic coordinate system. The pixels of peak powers are identified as IBs

a reference pixel (or pixels of reference area) is selected for the interpretation of the results. In our case the "stable" IB1 is selected as reference and its phase values are subtracted from IB2, IB3 and IB4 phase values. The relative velocities estimated by StaMPS are given in Table 1.

There is no need for great skill to conclude that these relative velocities cannot provide the displacement measured by GPS (Fig. 3). One might conclude that this technology doesn't work even in the presence of corner reflectors. Nevertheless, the LOS displacement series compared to GNSS derived LOS values can be used to reconstruct the displacement trends.

For the demonstration of manual procedure to correct the missing cycles the ascending IB4-IB1 data (between 26.04.2017 and 08.11.2017) were selected (Fig. 5). The curve of small circles presents the LOS displacements after the feasible unwrapping errors were numerically corrected. This correction significantly improved the velocity (~150 mm/y), but the curve is not as monotonic as it would be according to Fig. 3, and approximately -90 mm is missing to approach the GPS derived LOS displacement.

If the LOS displacements between two consecutive epochs are larger than the half wavelength (~28 mm), the

missing cycles cannot be computed similarly to unwrapping procedures. Nevertheless, the opposite movement (jumps), which does not fit to the overall tendency, may indicate the possible positions of missing half wavelength, which can be manually corrected. (In Fig. 5 three values were modified.) The manual correction is a usual method in practical InSAR applications [24].

After the manual corrections, when the InSAR and GPS derived LOS changes are as near as possible in the epochs of GPS measurements, the ASC curves are interpolated in the epoch of DSC curve and vice versa together with the epoch of starting and closing GNSS observations.

The interpolated ASC and DSC curves between two GPS measurements (starting with zero values) are given in Figs. 6 and 7. In the second interval the deformations are ~50% smaller.

After the manual corrections the differences between the InSAR and GPS derived LOS values are only few mm, typically less than 10 mm, therefor in the Kalman filter

Table 1 Relative velocities estimated by StaMPS

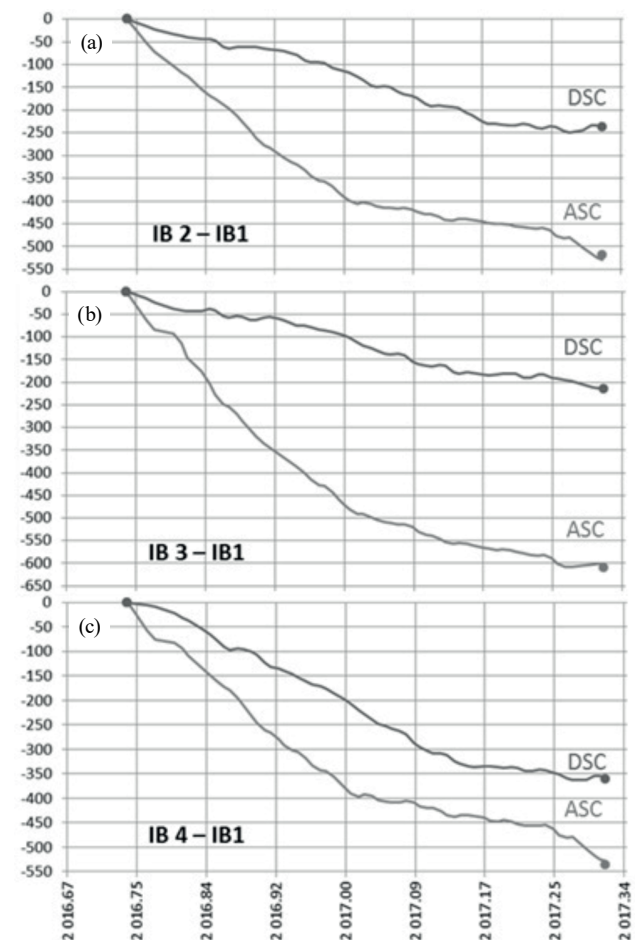| Time intervals:	28.09.2016 - 26.04.2017		26.04.2017 - 08.11.2017	
Orientation: velocity:	ascending (mm/year)	descending (mm/year)	ascending (mm/year)	descending (mm/year)
IB2 - IB1	-5.76	6.06	-13.5	-6.88
IB3 - IB1	-3.14	0.54	1.01	0.47
IB4 - IB1	-1.29	0.05	-2.02	-0.09
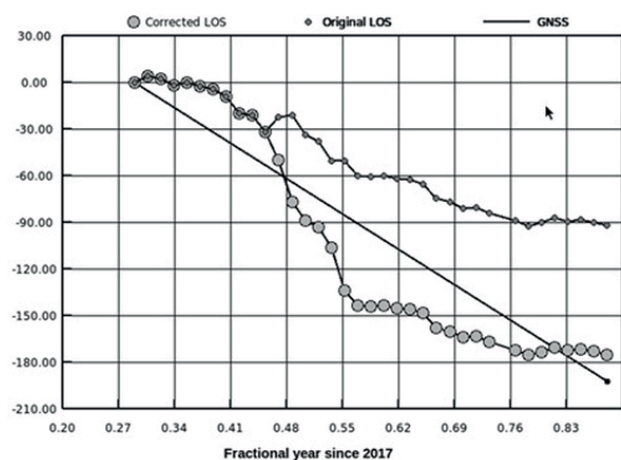
Fig. 5 Estimated and reconstructed LOS displacements of IB4-IB1 ascending curve and the linear GNSS trend (mm) between 26.04.2017 and 08.11.2017

Fig. 6 The interpolated ascending (ASC) and descending (DSC) curves (mm) between 28.09.2016 and 26.04.2017. The GPS derived values are signed by circles; (a) IB2–IB1, (b) IB3–IB1, (c) IB4–IB1 deformation values
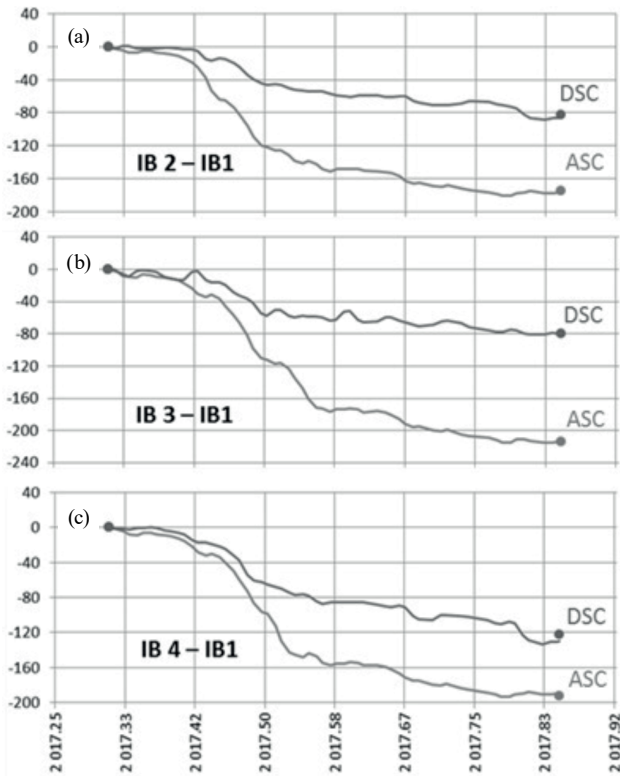
Fig. 7 The interpolated ascending (ASC) and descending (DSC) curves (mm) between 26.04.2017 and 08.11.2017. The GPS derived values are signed by circles; (a) IB2–IB1, (b) IB3–IB1, (c) IB4–IB1 deformation values
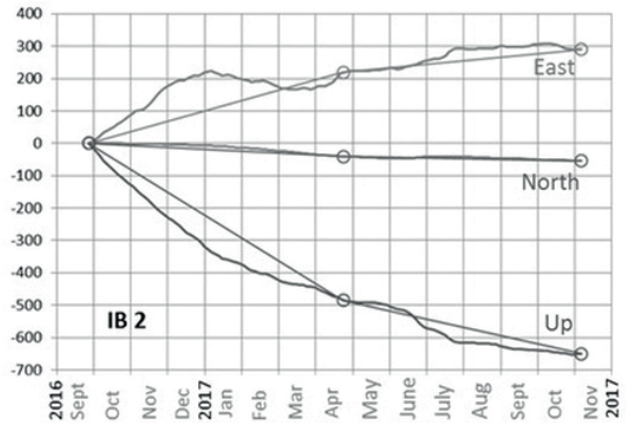

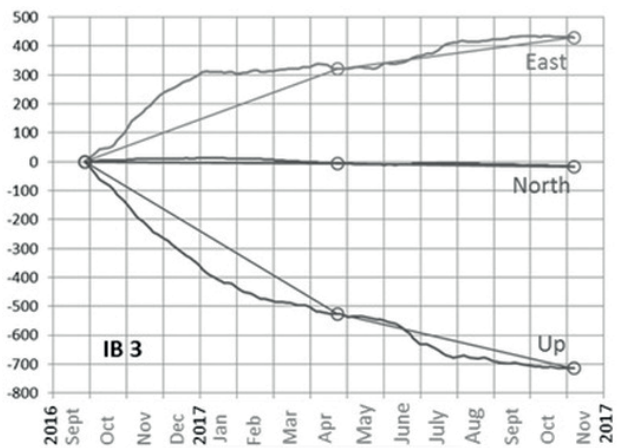Fig. 8 The estimated coordinate changes of IB2 (mm). The circles represent the GPS derived values

Fig. 9 The estimated coordinate changes of IB3 (mm). The circles represent the GPS derived values
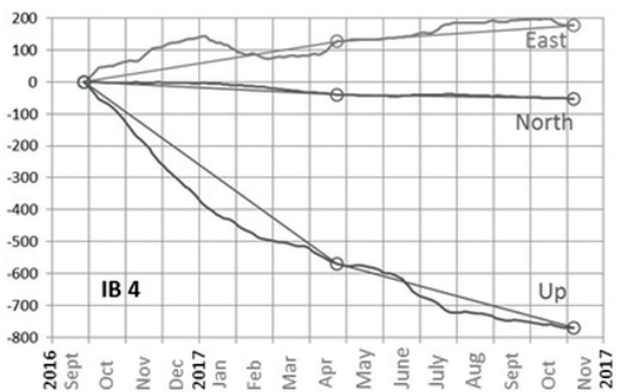

Fig. 10 The estimated coordinate changes of IB4 (mm). The circles represent the GPS derived values

procedure the estimated local coordinates (North, East and Up) are fitted to more accurate GPS derived displacements as boundary values.

The results of Kalman-filtering are plotted in Figs. 8–10 covering the whole investigated time period. It is clear that the north movements are basically provided by GPS observations and the straight lines are identical to those in Fig. 3.

4 Discussion

The velocities in the first period (Table 1) are similar to Kovács et al. [30], where two persistent scatterers were found south of the "Vár" hill indicated negative ASC and positive DSC velocities. During this investigation between 2014 and 2016 July, the IBs was not yet installed, therefore the results cannot be compared directly.

ISIGN processing revealed that there were missing half wavelengths in the relative curves, which could lead to the misinterpretation of the velocities. This is a consequence of the unwrapping errors and the movements larger than the half wavelength in the revisit cycle.

There were larger discrepancies in the first observation period, but fortunately it was possible to recover the curves by manually correcting the unwrapped deformations. This

is of course not an exact solution, but our former experiences were used to provide feasible solution. In the second period only, a few manual steps were needed which is the consequence of the decelerated movements. In the case of more rapid movements the InSAR technologies cannot be used at all.

The main point of the ISIGN procedure is the use of GNSS observations which provides the boundary values for the Kalman-filter. Since the ascending and descending displacements are not sensitive to the north movements the north components are estimated basically by GNSS observation. Fortunately, in this case the north component of the deformations are small (1–5 cm).

The GPS derived curves (Fig. 3) indicate the deceleration of the movements in the last two periods and the estimated curves (Figs. 8–10) fit to the GPS data.

Both the East and Up (vertical) curves indicate different movement tendencies, which cannot be described by one average velocity.

In the case of Up components four subsidence periods can be distinguished at all points:

1. 2016 Oct – 2016 Jan: nearly linear fast movements,
2. 2016 Feb – 2017 May: nearly linear, but slower movements,
3. 2017 June–July: acceleration of the movements,
4. 2017 Aug–Oct: deceleration to nearly stationary state.

In the case of smaller East components, the curves are more complex:

1. 2016 Oct–Dec: nearly linear fast movements at all points,
2. 2017 Jan–Apr: opposite movements started, then retained at points IB2 and IB4,
3. 2017 Jan–June: very small linear movements at point IB 3,
4. 2017 July-Oct: after a short growth very small movements nearly to the stationary state at all points.

The contradictory movements of points IB 2 and IB 4 in the East components may be explained by the tilt of the creeping plate affecting the escape of the deep plastic materials into the Danube.

5 Conclusions

The integrated benchmarks (Fig. 2) and the ISIGN procedure proved to be a useful approach to investigate landslides, or other surface deformations, where the traditional InSAR processing cannot be applied. The combination of a sparse GNSS observation and the processing of more frequent Sentinel-1 images compensate their disadvantages. The GNSS measurements can be used to identify the pixels dominated by IBs; to provide the boundary values of Kalman-filtering and estimate the north movements, which cannot be determined by InSAR technologies.

If the movements are partly larger than the half wavelength between two consecutive epochs the manual steps may help to reconstruct the movement process. Of course, it does not work if the changes are very fast, but the results of GNSS measurements can be used itself, as well.

Despite the very sophisticated InSAR technologies the results may be misleading if there is no proper field control. Fortunately, the north components are the smallest in this area; however, there may be more significant in other cases.

The six-day repeat cycle of Sentinel-1 satellites provides a detailed movement history, which demonstrated several movement periods of Up (vertical) and East component that are very useful in the geomorphologic interpretation of the landslides.

In the case of important and endangered areas the introduced procedure may be a useful monitoring technology:

- At the first step optimal IBs network should be planned, established and initially measured by GNSS network technology.
- In the next step the SAR images can be processed.
- If the InSAR processing indicates probable movements, the GNSS network observations have to be repeated and the data processing have to be carried out.
- The last two steps need to be repeated according to the experienced movements.

The repeat cycle of GNSS network observation depend on the magnitude of experienced movements, which ensures minimal user interactions during the data processing.

During the network planning it is reasonable to study several important aspects:

- fracture zone investigation to define stable and potentially moving parts,
- estimation of average normalized radar background power using available Sentinel-1 images.
- control of GNSS satellite configuration and the visibility of ASC and DSC Sentinel-1 passes.

References

[1] National Cadaster of Surface Movements, Budapest, Hungary [online] Available at: https://mbfsz.gov.hu

[2] Lóczy, D., Balogh, J., Ringer, Á. "Landslide hazard induced by river undercutting along the Danube", [pdf] Geomorphological Hazards, Supplements of Geografia Fisica e Dinamica Quaternaria, II, pp. 5–11, 1989. Available at: http://www.glaciologia.it/wp-content/uploads/Supplementi/FullText/SGFDQ_II_1989_FullText/02_SGFDQ_II_1989_Loczy_5_11.pdf

[3] Lóczy, D., Kertész, Á., Lóki, J., Kiss, T., Rózsa, P., Sipos, Gy., Sütő, L., Szabó, J., Veress, M. "Recent Landform Evolution in Hungary", In: Lóczy, D., Stankoviansky, M., Kotarba, A. (eds.) Recent Landform Evolution – The Carpatho–Balkan–Dinaric Region, Springer, 2012, pp. 205–247. ISBN: 978-94-007-2447-1
https://doi.org/10.1007/978-94-007-2448-8_9

[4] Domján, J. "Középdunai magaspartok csúszásai" (Slides of the bluffs along the middle reach of the River Danube), [pdf] Hidrológiai Közlöny, 32, pp. 416–422, 1952. Available at: https://adt.arcanum.com/en/view/HidrologiaiKozlony_1952/?pg=441&layout=s (in Hungarian)

[5] Kézdi, Á. "A dunaújvárosi partrogyás" (The bank collapse at Dunaújváros), Mélyépítéstudományi Szemle, 20, pp. 281–297, 1970. (in Hungarian)

[6] Horváth, Zs., Scheuer, Gy. "A dunaföldvári partrogyás mérnökgeológiai vizsgálata" (Engineering geological investigation of the bank collapse at Dunaföldvár), Földtani Közlöny, 106, pp. 425–440, 1976. (in Hungarian with German abstract)

[7] Pécsi, M., Scheuer, Gy. "Engineering geological problems of the Dunaújváros loess bluff", Acta Geologica Hungarica, 22, pp. 345–353, 1979.

[8] Pécsi, M., Schweitzer, F., Scheuer, Gy. "Engineering geological and geomorphological investigations of landslides in the loess bluffs along the Danube in the Great Hungarian Plain", Acta Geologica Hungarica, 22, pp. 327–343, 1979.

[9] Juhász, Á. "A klimatikus hatások szerepe a magaspartok fejlődésében" (Role of climatic effects in the development of high banks), Földtani Kutatás, 36, pp. 14–20, 1999. (in Hungarian)

[10] Kleb, B., Schweitzer, F. "A Duna csuszamlásveszélyes magaspartjainak településkörnyezeti hatásvizsgálata" (Assessment of the impact of landslide prone high banks on urban environment along the River Danube), In: Ádám, A., Meskó, A. (eds.) Földtudományok és a földi folyamatok kockázati tényezői, Magyar Tudományos Akadémia, Budapest, Hungary, 2001, pp. 169–193. (in Hungarian) ISBN: 963-508-317-3

[11] Szabó, J. "The relationship between landslide activity and weather: examples from Hungary", Natural Hazards and Earth System Sciences, 3, pp. 43–52, 2003.
https://doi.org/10.5194/nhess-3-43-2003

[12] Kraft, J. "Dunai magaspart dunaszekcsői részletének rogyásos suvadásai" (Slumping of Danube's high bank at Dunaszekcső), In: Török, Á., Vásárhelyi, B. (eds.) Mérnökgeológia–Kőzetmechanika, Műegyetemi Kiadó, Budapest, Hungary, 2011, pp. 1–12. (in Hungarian) ISBN: 9786155086045

[13] Karbon, M., Brückl, E., Hegedűs, E., Preh, A. "Kinematics of a mass movement constrained by sparse and inhomogeneous data", Natural Hazards and Earth System Sciences, 11(6), pp. 1609–1618, 2011.
https://doi.org/10.5194/nhess-11-1609-2011

[14] Újvári, G., Mentes, Gy., Bányai, L., Kraft, J., Gyimóthy, A., Kovács, J. "Evolution of a bank failure along the River Danube at Dunaszekcső, Hungary", Geomorphology, 109, pp. 197–209, 2009.
https://doi.org/10.1016/j.geomorph.2009.03.002

[15] Bányai, L., Mentes, Gy., Újvári, G., Kovács, M., Czap, Z., Gribovszki, K., Papp, G. "Recurrent landsliding of a high bank at Dunaszekcső, Hungary: Geodetic deformation monitoring and finite element modeling", Geomorphology, 210, pp. 1–13, 2014.
https://doi.org/10.1016/j.geomorph.2013.11.032

[16] Bányai, L., Szűcs, E., Wesztergom, V. "Geometric features of LOS data derived by SAR PSI technologies and the three-dimensional data fusion", Acta Geodaetica et Geophysica, 52(3), pp. 421–436, 2016.
https://doi.org/10.1007/s40328-016-0183-3

[17] Wright, T. J., Parsons, B. E., Lu, Z. "Toward mapping surface deformation in three dimensions using InSAR", Geophysical Research Letters, 31(1), pp. 1–5, 2004.
https://doi.org/10.1029/2003GL018827

[18] Hung, W.-C., Hwang, C., Chen, Y.-A., Chang, C.-P., Yen, J.-Y., Hooper, A., Yang, C.-Y. "Surface deformation from persistent scatterers SAR interferometry and fusion with leveling data: A case study over the Choushui River Alluvial Fan, Taiwan", Remote Sensing of Environment, 115, pp. 957–967, 2011.
https://doi.org/10.1016/j.rse.2010.11.007

[19] García-Davalillo, J. C., Herrera, G., Notti, D., Strozzi, T., Álvares-Fernandez, I. "DInSAR analysis of ALOS PALSAR images for the assessment of very slow landslides: the Tena Valley case study", Landslides, 11, pp. 225–246, 2014.
https://doi.org/10.1007/s10346-012-0379-8

[20] Hu, J., Li, Z. W., Ding, X. L., Zhu, J. J., Zhang, L., Sun, Q. "Resolving three-dimensional surface displacements from InSAR measurements: A review", Earth-Science Reviews, 133, pp. 1–17, 2014.
https://doi.org/10.1016/j.earscirev.2014.02.005

[21] Ferretti, A. "Satellite InSAR Data: Reservoir Monitoring from Space (EET 9)", EAGE Publication, 2014. ISBN: 9073834716
https://doi.org/10.3997/9789073834712

[22] Barra, A., Monserat, O., Mazzanti, P., Esposito, C., Crosetto, M., Mugnozza, G. S. "First insights on the potential of Sentinel-1 for landslides detection", Geomatics, Natural Hazards and Risk, 7(6), pp. 1874–1883, 2016.
https://doi.org/10.1080/19475705.2016.1171258

[23] Bayer, B., Simonia, A., Schmidt, D., Bertelloa, L. "Using advanced InSAR techniques to monitor landslide deformations induced by tunneling in the Northern Apennines, Italy", Engineering Geology, 226(30), pp. 20–32, 2017.
https://doi.org/10.1016/j.enggeo.2017.03.026

[24] Parker, A. L. "InSAR Observations of Ground Deformation - Application to the Cascades Volcanic Arc", Springer, 2017. ISBN: 978-3-319-39033-8
https://doi.org/10.1007/978-3-319-39034-5

[25] Cianflone, G., Tolomei, C., Brunori, C. A., Monna, S., Dominici, R. "Landslides and Subsidence Assessment in the Crati Valley (Southern Italy) Using InSAR Data", Geosciences, 8(2), 67, 2018.
https://doi.org/10.3390/geosciences8020067

[26] Solari, L., Raspini, F., Del Soldato, M., Bianchini, S., Ciampalini, A., Ferrigno, F., Tucci, S., Casagli, N. "Satellite radar data for back-analyzing a landslide event: the Ponzano (Central Italy) case study", Landslides, 15(4), pp. 773–782, 2018.
https://doi.org/10.1007/s10346-018-0952-x

[27] Rosi, A., Tofani, V., Tanteri, L., Tacconi Stefanelli, C., Agostini, A., Catani, F., Casagli, N. "The new landslide inventory of Tuscany (Italy) updated with PS-InSAR: geomorphological features and landslide distribution", Landslides, 15(1), pp. 5–19, 2018.
https://doi.org/10.1007/s10346-017-0861-4

[28] Consiglio Nazionale Delle Ricerche "DORIS project" [online] Available: http://www.doris-project.eu

[29] Raventós, J., Sánches, J., Fusi, B. "The use of InSAR as a tool to assess ground deformation: the cases of Rácalmás and Dunaszecksó, Hungary", ce/papers, Special Issue: XVI DECGE 2018 Proceedings of the 16th Danube - European Conference on Geotechnical Engineering, 2 (2–3), pp. 243–248, 2018.
https://doi.org/10.1002/cepa.678

[30] Kovács, I. P., Bugya, T., Czigány, Sz., Defilippi, M., Lóczy, D., Riccardi, P., Ronczyk, L., Pasquali, P. "How to avoid false inter-pretations of Sentinel-1A TOPSAR interferometric data in land-slide mapping? A case study: recent landslides in Transdanubia, Hungary", Natural Hazards, 96, pp. 693–712, 2019.
https://doi.org/10.1007/s11069-018-3564-9

[31] Szalai, S., Szokoli, K., Metwaly, M. "Delineation of landslide endangered areas and mapping their fracture systems by the pres-sure probe method", Landslides, 11, pp. 923–932, 2014.
https://doi.org/10.1007/s10346-014-0509-6

[32] Szokoli, K., Szarka, L., Metwaly, M., Kalmár, J., Prácser, E., Szalai, S. "Characterisation of a landslide by its fracture system using Electric Resistivity Tomography and Pressure Probe meth-ods", Acta Geodaetica et Geophysica, 53, pp. 15–30, 2018.
https://doi.org/10.1007/s40328-017-0199-3

[33] Szederkényi, T. "A baranyai Duna menti mezozoós szigetrögök földtani viszonyai" (Geological conditions of the Mesozoic blocks along the River Danube in county Baranya), [pdf] Földtani Közlöny, 94(1), pp. 27–32, 1964. Available at: https://epa.oszk.hu/01600/01635/00169/pdf/EPA01635_foldtani_kozl-ony_1964_094_1_027-032.pdf (in Hungarian with German abstract)

[34] Urbancsek, J. "Magyarország mélyfúrású kútjainak katasztere, VII" (Cadastre of the deep–drilling wells in Hungary VII), Víz-gazdálkodási Intézet, Budapest, Hungary, 1977. (in Hungarian)

[35] Moyzes, A., Scheuer, Gy. "A dunaszekcsői magaspart mérnök-geológiai vizsgálata" (Engineering geological investigation of the high bank at Dunaszekcső), [pdf] Földtani Közlöny, 108(2), pp. 213–226, 1978. Available at: http://real-j.mtak.hu/8920/2/Foldtani_Kozlony_1978_108_2.pdf (in Hungarian with German abstract)

[36] Rónai, A. "The Quaternary of the Great Hungarian Plain", In: Pécsi, M. (ed.) Loess and the Quaternary: Chinise and Hungarian case studies, Akadémiai Kiadó, Budapest, Hungary, 1985, pp. 51–63. ISBN: 9630542277

[37] Hegedűs, E., Kovács, A. Cs., Fancsik, T. "A megcsúszott dunasze-kcsői löszfal aktív és passzív szeizmikus vizsgálata" (Active and passive seismic investigation of the slipped loess bluff at Dunaszekcső), Research Report of the Eötvös Loránd Geophysical Institute, Hungary, 2008.

[38] Bányai, L., Nagy, L., Hooper, A., Bozsó, I., Szűcs, E., Wesztergom, V. "Investigation of Integrated Twin Corner Reflectors Designed for 3-D InSAR Applications", IEEE Geoscience and Remote Sensing Letters, 17(6), pp. 1013–1016, 2020.
https://doi.org/10.1109/LGRS.2019.2939675

[39] Bozsó, I., Bányai, L., Hooper, A., Szűcs, E., Wesztergom, V. "Integration of Sentinel-1 Interferometry and GNSS Networks for Derivation of 3-D Surface Changes", IEEE Geoscience and Remote Sensing Letters, 18(4), pp. 692–696, 2021.
https://doi.org/10.1109/LGRS.2020.2984917

[40] Werner, C., Wegmüller, U., Strozzi, T., Wiesmann, A. "Gamma SAR and Interferometric Processing Software", [pdf] presented at ERS-ENVISAT Symposium, Gothenburg, Sweden, 16–20 Oct. 2000. Available at: https://www.gamma-rs.ch/uploads/media/2000-1_GAMMA_Software.pdf

[41] Hooper, A., Bekaert, D., Spaans, K., Arıkan, M. "Recent advances in SAR interferometry time series analysis for measuring crustal deformations", Tectonophysics, 514–517, pp. 1–13, 2012.
https://doi.org/10.1016/j.tecto.2011.10.013